TIME-DOMAIN CHARACTERIZATION OF SAW DEVICES

Robert C. Bray
Tim L. Bagwell
Roger L. Jungerman
Scott S. Elliott

Hewlett-Packard
Microwave Technology Division
1412 Fountaingrove Parkway
Santa Rosa, CA 95401

RF & Microwave Measurement Symposium and Exhibition

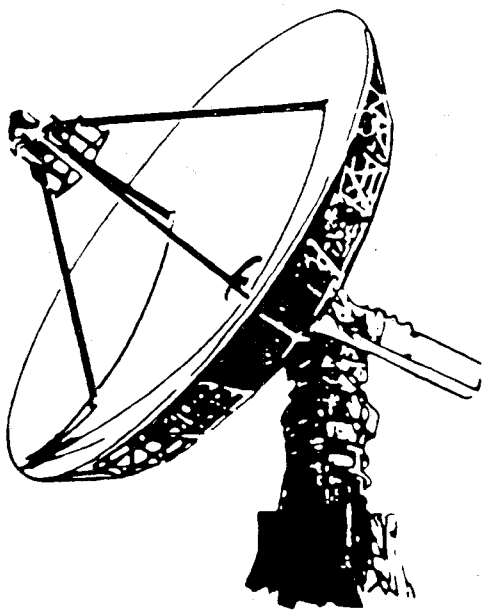

HEWLETT PACKARD

Time Domain Characterization of SAW Devices

Surface Acoustic Wave (SAW) devices have assumed increasing importance as signal processing components in the frequency range 20 MHz to 2 GHz. SAW resonators, filters, and delay lines offer performance unachievable by other means, and are attractive for their small size, repeatable characteristics, and low cost. Characteristic SAW device specifications include insertion loss, bandwidths, out-of-band rejection, group delay ripple, input and output impedances, and phase linearity. These are straightforward measurements with a network analyzer with sufficient frequency accuracy and dynamic range. SAW devices are all fundamentally based on the delay of acoustic signals travelling 5 orders of magnitude slower than electromagnetic signals. Ideal device response is shown to be degraded by spurious acoustic reflections in the device, which are a key limitation on device performance. The built-in time domain capability of the HP 8753A network analyzer is shown to be an indispensable tool for complete analysis of device response including time spurious.

Bob Bray, Project Manager, Physical Wave Device R&D, HP Microwave Technology Division, Santa Rosa, CA. B.S., M.S., Physics, University of Michigan, 1966., 1967. Taught high school physics, 1969-1977. MSEE, Ph.D., Stanford University, 1979, 1981. Thesis work in acoustic and photoacoustic microscopy. Joined HP in 1981, where he has been involved with R&D in acoustic and optical devices.

Tim Bagwell, R&D Engineer, HP Microwave Technology Division, Santa Rosa, CA. BSEE, University of Illinois, 1980. Joined HP in 1980. Worked on HP 853A spectrum analyzer, and on millimeter-wave device characterization. In 1983-84, worked on the antiproton source at Fermilab, Batavia, Illinois. Returned to HP in 1984, where he has since been involved in acoustic wave device R&D.

Roger Jungerman, R&D Engineer, HP Microwave Technology Division, Santa Rosa, CA. B.A. Physics, University of California, Santa Cruz, 1978. With Watkins-Johnson Co., 1978-1981, working on thin film coatings. M.S., Ph.D, Applied Physics, Stanford University, 1983, 1985, where thesis work concerned scanning optical microscopy, fiber optics, and acoustics. Joined HP in 1985, where he has been involved with acoustic and optical device R&D.

Scott Elliott, Section Manager, Wave Technology R&D, HP Microwave Technology Division, Santa Rosa, CA. BSEE, MSEE, University of California, Berkeley, 1969, 1971. Worked with several firms in microwave devices, 1971-1975. Ph.D., University of California, Santa Barbara, 1978, with thesis work in acoustic imaging. With HP since 1978, working on GaAs FETs, acoustic devices, millimeter wave integrated circuits, and optics.

1. INTRODUCTION TO SAW TECHNOLOGY
2. SAW DEVICE MEASUREMENTS IN FREQUENCY AND TIME DOMAINS
   A. FILTERS
   B. DELAY LINES
   C. RESONATORS
3. CONCLUSION

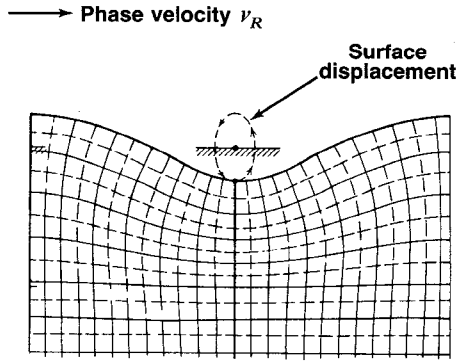

Surface acoustic waves can exist on the free surfaces of solids. The natural waveguiding of the free surface allows a wave whose particle motion at the surface is a retrograde ellipse [4,5] These waves exist as one of the components of earthquakes (the L wave or slowest to arrive) where they have wavelengths measured in kilometers and frequencies of fractions of 1 Hz. They were predicted to exist by Lord Rayleigh in 1885, and experimentally observed 20 years later [1]. The same type of wave on a crystalline substrate is the basis of SAW device technology, which has grown rapidly since its origin in 1965 [2].

SAW SURFACE CONFINEMENT

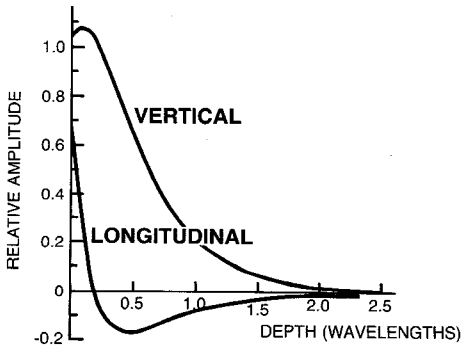

The free surface of a crystalline solid provides a natural waveguide for SAWs. The amplitude decays exponentially into the interior of the substrate for both the vertical and longitudinal components of the motion. Note that most of the energy is trapped within 1 wavelength of the surface [4,5]. This has the great advantage of access to signal processing elements which can be fabricated easily on the exposed surface.

ACOUSTIC ATTENUATION
IN GASES, LIQUIDS & SOLIDS

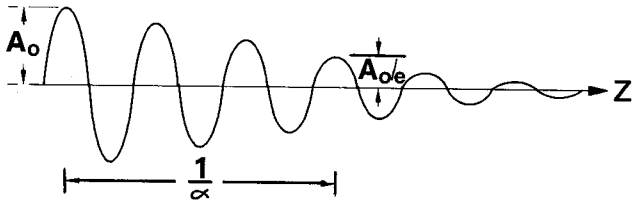

$$A(t,z) = A_o \cos(kz - wt) e^{-\alpha z}$$

For most conditions, 1 medium

$$\frac{\alpha}{f^2} = \text{Constant}$$

A sound wave of any type is attenuated as it travels through any medium, by scattering or viscous damping, for example. In a given medium the attenuation constant is typically proportional to the square of the frequency.

ATTENUATION EXAMPLES
(f = 100 MHz)

MATERIAL	ATTENUATION	WAVE TYPE
Air, STP	2000 dB/mm	Longidudinal
Water	3 dB/mm	Longitudinal
ST-Quartz	.008 dB/mm	SAW
YZ-$LiNbO_3$	.002 dB/mm	SAW

For representative media, the 100 MHz sound attenuation values are shown here. Notice that in crystalline solids the attenuation for SAWs is orders of magnitude lower than for longitudinal sound waves in liquids and gases. This is the fundamental material property that makes SAW technology possible [4,6].

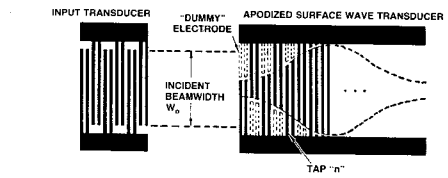

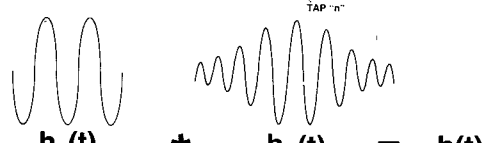

$h_1(t) * h_2(t) = h(t)$

$H_1(f) \bullet H_2(f) = H(f)$

A SAW filter chip exhibits features common to all SAW devices. It consists of a piezoelectric substrate upon which input and output interdigital transducers (IDTs) are deposited. The IDTs, which are metal electrodes connected to two bus bars as shown, convert electrical signals to surface acoustic waves and vice versa at the input and output of the device. Bidirectional transducers launch SAW energy in both directions. Each electrode in a bidirectional transducer is split to suppress internal reflections within the transducer. The split elctrodes are one eighth wavelength wide, separated by one eighth wavelength. The impulse responses of the two transducers are shown in the center of the figure. Notice the correspondence between envelope of the impulse response and the overlap pattern of the fingers in the transducers. The convolution of these impulse responses gives the overall filter impulse response. The frequency response of the transducer is obtained by multiplying the Fourier Transforms of the impulse responses, apart from a phase factor due to the acoustic delay. Acoustic propagation loss must be considered at high frequencies [4,7].

NASTY REALITIES OF SAW

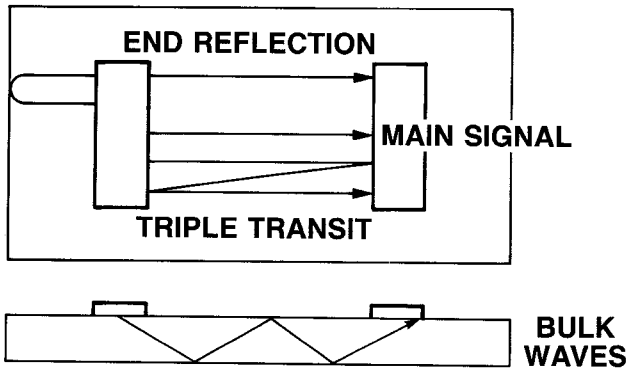

Some of the nasty realities (time spurious) encountered with SAW devices are indicated in this slide. Waves launched towards the end of the substrate out the back of the transducer will be reflected towards the output transducer if an absorbing layer is not deposited to suppress them. The triple transit signal is a major time spurious and a major source of passband ripple. Its level is sensitive to electrical matching conditions and is thus adjustable by the circuit designer employing the SAW device. Direct electromagnetic coupling is a source of time spurious and passband ripple as well. It can be reduced by increasing the delay path and by careful packaging design. Interdigital transducers also launch longitudinal and shear waves into the bulk of the crystal substrate, where they may reflect back to the output transducer, causing a spurious response, typically at frequencies higher than the SAW passband.

SAW TRANSDUCER EQUIVALENT CIRCUIT

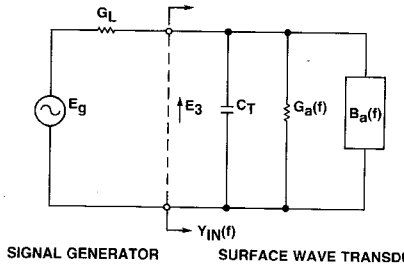

Where: C_T = static IDT capacitance
Ga(f) = acoustic radiation conductance
Ba(f) = acoustic susceptance

A SAW transducer at its simplest may be represented by the equivalent circuit shown here. Ct represents the interdigital static capacitance, which is independent of frequency. Ga is the acoustic radiation conductance, representing SAW energy launched away from the transducer. Its frequency dependence is corresponds to that outlined before. Ba represents non-radiating energy storage asociated with the acoustic excitation of the transducer [5].

SAW Technology – Why?

- 20 years old
- Unique signal processing
  20 MHz – 2 GHz+
- Low loss for acoustics in crystalline solids
- Piezoelectric coupling to circuits
- An IC-like technology
  - *Repeatable process
  - *Small, easy to mass produce
  - *Inexpensive

SAW device technology is barely 20 years old. It has developed rapidly because it makes possible unique signal processing capabilities in the frequency range 20 MHz - 2 GHz. The lower limit is set by impractically large device size and availibility of alternatives. At frequencies much above 1 GHz optical lithography is no longer feasible, as the transducer fingers drop below 1 micron in width. The technology is based on the fact that SAWs in the RF, UHF, and low microwave frequency ranges experience low propagation loss in crystalline solids such as quartz and lithium niobate that are piezoelectric and thus can couple electrical energy to acoustic energy. SAW device fabrication is an integrated circuit - like technology, where many small, easy to mass produce chips may be produced on a single wafer.

SAW DEVICE TYPES

- Bandpass Filters
  - *Undirectional: low loss
  - *Bidirectional: precise shape
- Delay lines
- Resonators
- Multipole resonators
- Dispersive delay lines
- Matched filters
- Storage correlators

Many types of signal processing devices may be fabricated with SAW technology. In this paper we examine measurements necessary to characterize two types of SAW bandpass filters, as well as delay lines and resonators.

HIGH-VOLUME SAW APPLICATIONS

* TV IF Filters
* Garage door openers
* CATV set-top converters
* SAW wireless labels?

SAW FILTER RESPONSE

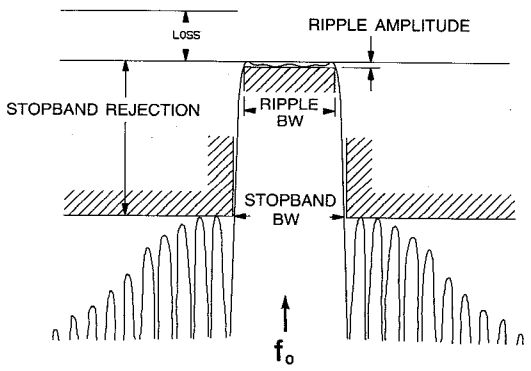

SAW filters for different applications have a variety of very demanding performance requirements. This results in the need to measure several aspects of the filters' frequency and time domain responses. These measurement needs are not only present in the design process but also in the manufacturing of such devices. Typical SAW filter specifications are insertion loss, ripple bandwidth, stopband bandwidth, stopband rejection, passband ripple amplitude, phase ripple amplitude, phase linearity, and group delay. Additionally, The more demanding applications require minimizing time spurious signals resulting in specifications in the time domain as well as those in the frequency domain listed above.

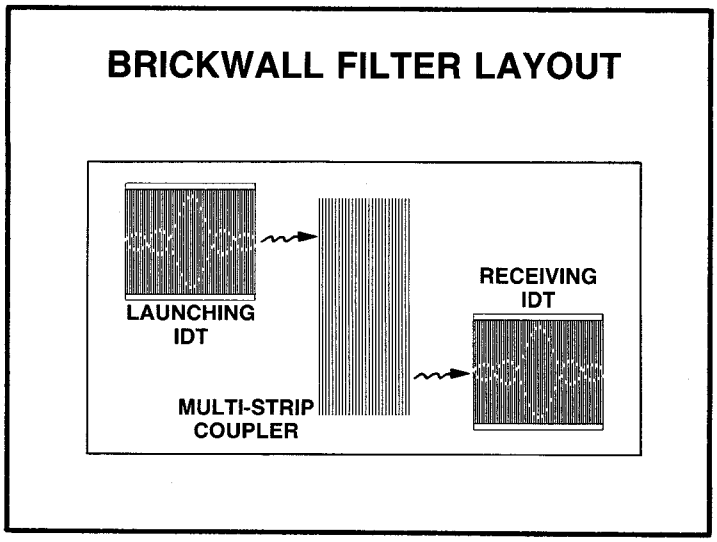

A brickwall filter is one with a shape factor approaching unity. These filter shapes are usually designed to yield the maximum possible passband bandwidth while providing adequate rejection of spurious signals such as the feedthrough of a local oscillator. A typical application is to provide adjacent channel and spurious rejection at an IF frequency. Almost all television tuners now manufactured in the world contain a SAW IF filter of this type for adjacent-channel rejection. Brickwall filters are typically designed with two bidirectional apodized IDTs, of the split finger type, coupled via a multi-strip coupler. The use of an MSC allows higher stopband rejection per device since two apodized IDTs can be used. Another advantage of the MSC design is that the IDTs can be offset transversely from one another, thus reducing coupling to bulk modes.

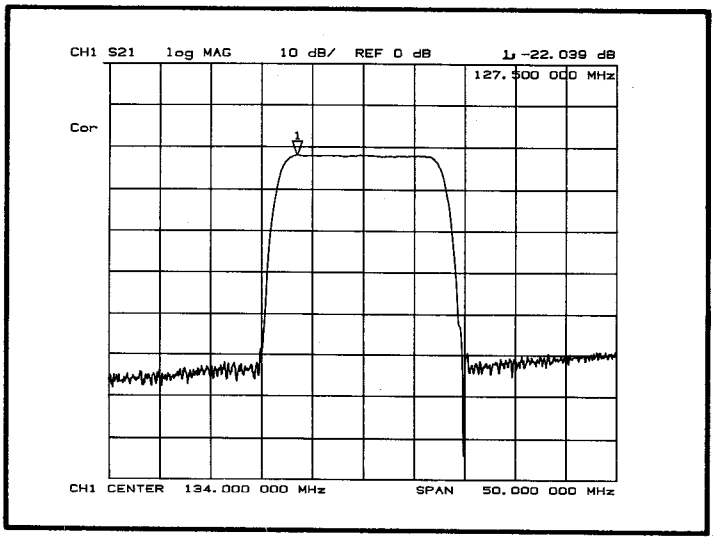

The frequency response of a typical brickwall filter is shown in this figure. In order to improve the dynamic range of the instrument, the IF bandwidth was reduced to 30 Hz. Marker 1, positioned at the peak of the response, shows a minimum insertion loss of 22.04 dB. The stopband rejection can be seen to be about 50 dBc.

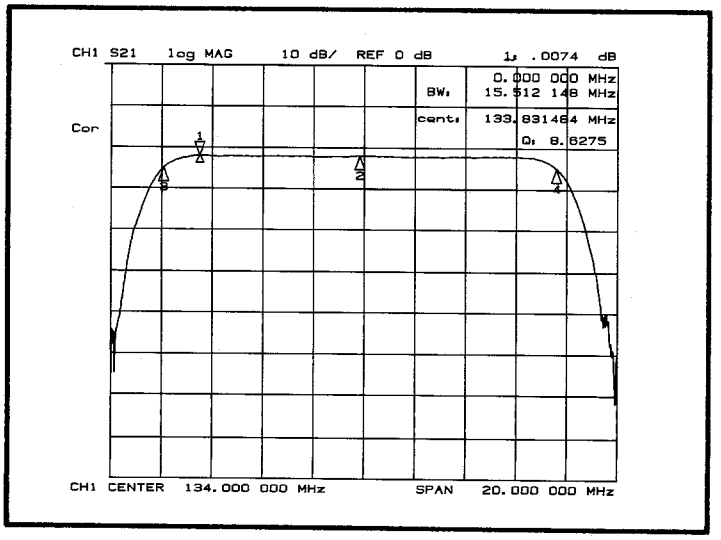

This figure shows the filter passband. Here marker 1 has been zeroed so that the marker width search feature can be used to determine the 3 dB bandwidth. Markers 3 and 4 are positioned at points 3 dB lower than marker 1. The user can immediately read the 3 dB bandwidth which is 15.51 MHz. The center frequency of the filter has also been computed as the average of the 3 dB frequencies and can be seen to be 133.83 MHz.

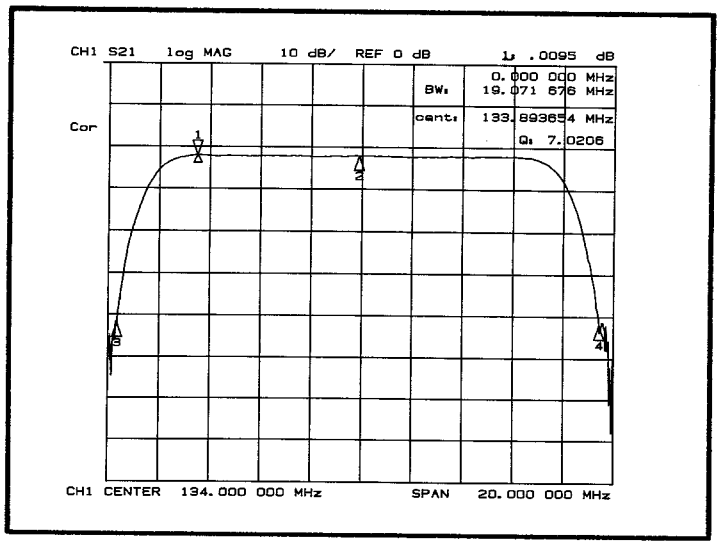

The 40 dB bandwidth, of 19.07 MHz, is just as easily obtained using the marker width search feature. The shape factor can now be computed as the ratio of the 40 dB bandwidth to the 3 dB bandwidth which gives a shape factor of 1.23 for this filter. Such a shape factor is routinely achievable with SAW filters due to their transversal character [4,5].

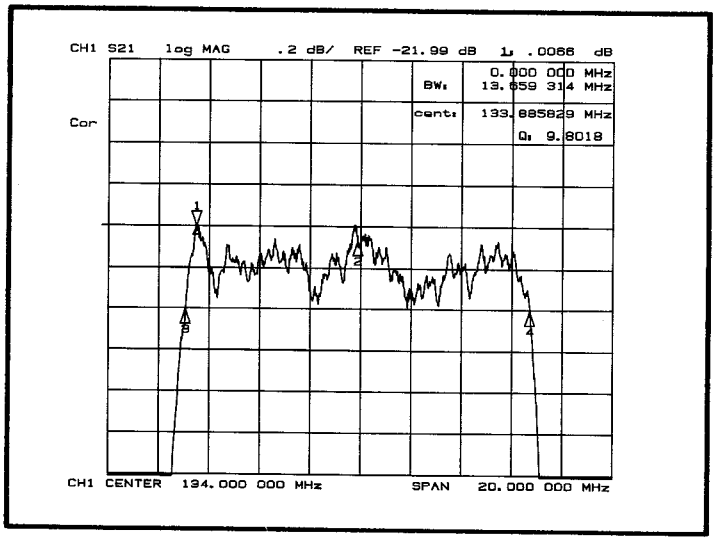

Reducing the scale to 0.2 dB/div allows the passband ripple to be measured. Here marker 1 has been used to shift the peak of the response to the reference line. The ripple amplitude is seen to be about 0.4 dB peak to peak. It is a common practice with brickwall filters to specify the ripple bandwidth. This bandwidth is defined to be the width of the response where the amplitude is reduced by an amount equal to the peak to peak ripple amplitude. Again using the marker width search feature to find the 0.4 dB bandwidth, the ripple bandwidth is found to be 13.66 MHz.

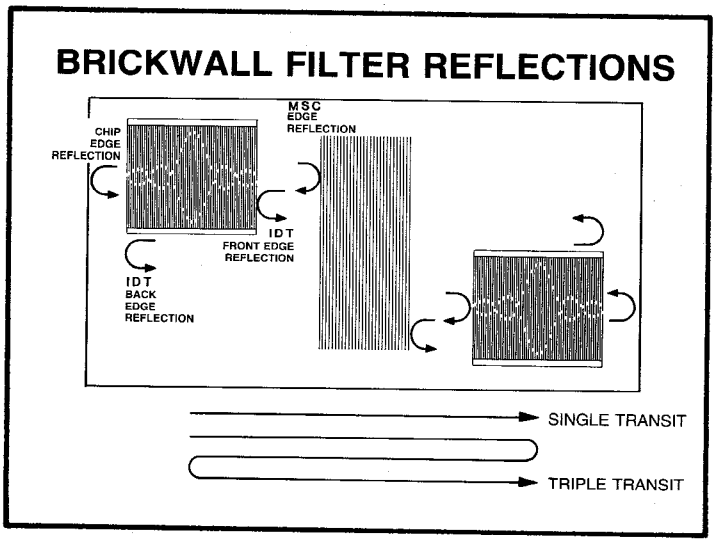

Three different ripple periods dominate the passband response. The ripple with the shortest period is due to beating between the single transit acoustic signal and the triple transit acoustic signal. An approximate formula for computing this ripple period is given by $p = v/(2L)$ where p is the period in Hz, v is the acoustic velocity in meters/second, and L is the center to center distance between IDTs in meters. One can also see a ripple component which is about twice that of the triple transit ripple. This ripple is due to beating between the acoustic signal and the electromagnetic feedthrough signal which is coupled between the IDTs through stray parasitic capacitance. The approximate period of this ripple can be computed from $p = v/L$. The longest period ripple component is Fresnel ripple due to truncation of the IDT samples. It is related to the length of the IDT and the number of fingers in the IDT.

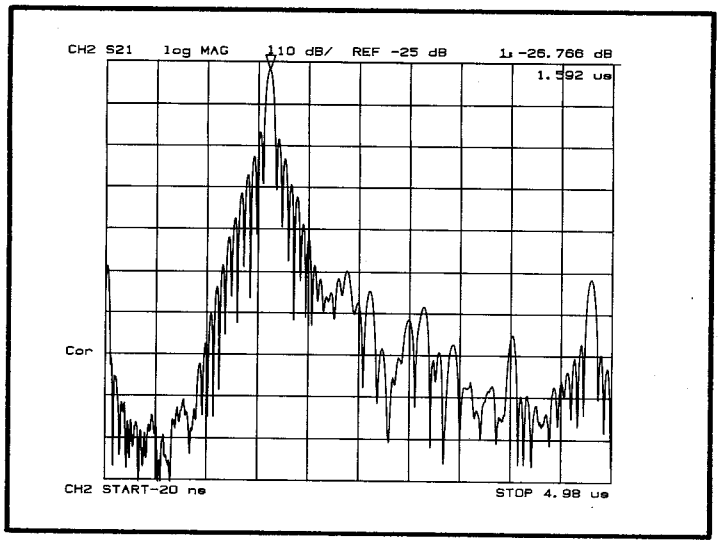

The time domain transformation capability is an indispensable tool for analyzing SAW filters. Here an 801 point transform has been performed. It is important to adjust the frequency sweep to give the proper time domain resolution. The simple formula for determining the time domain resolution is t = 1/span where t is the time resolution in microseconds, and span is the frequency span in Mhz. In this case,the span is 50 Mhz which gives a time resolution of 20 nsec. The time resolution should be adjusted to give adequate sampling of the finest detail of interest in the time response. The time response shows the computed impulse response for S21. Here again an IF bandwidth of 30 Hz has been selected to improve the dynamic range of the instrument. A great deal of information can be gathered about the filters performance from the time response. Most notable is the impulse response of the single transit signal at 1.592 usec. This is an approximate picture of the convolution of the apodization pattern of the launching and receiving transducers. The electromagnetic feedthrough at 0 usec can also be observed to be approximately 47 dBc. At 4.78 uS, the triple transit signal is observed to be about 50dBc. These two time spurious signals are responsible for most of the fast passband ripple. In addition to these signals, many other spurious signals can be observed in the region between the single transit and the triple transit signals. These signals are due to acoustic reflections from various interfaces such as IDT front and back edges, MSC front and back edges, chip edges and others. By determining the times of these spurious reflections and knowledge of the device layout, one can determine the source of the various reflections.

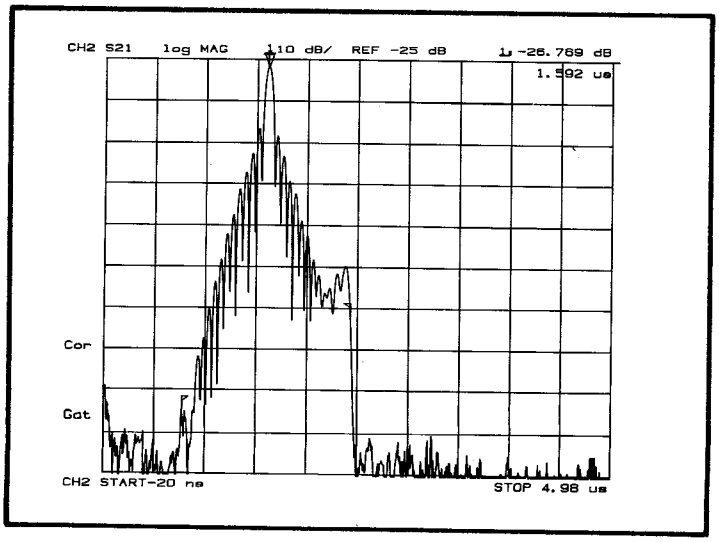

Another powerful feature of the HP 8753A is the time domain gating capability. This capability allows the user to gate out the spurious time signals in order to determine the filters frequency response without the interfering spurious signals. By placing the gate center at the peak of the time response and adjusting the gate span to include all of the filter sidelobes, we can perform an inverse transform of the gated data to obtain the idealized frequency response.

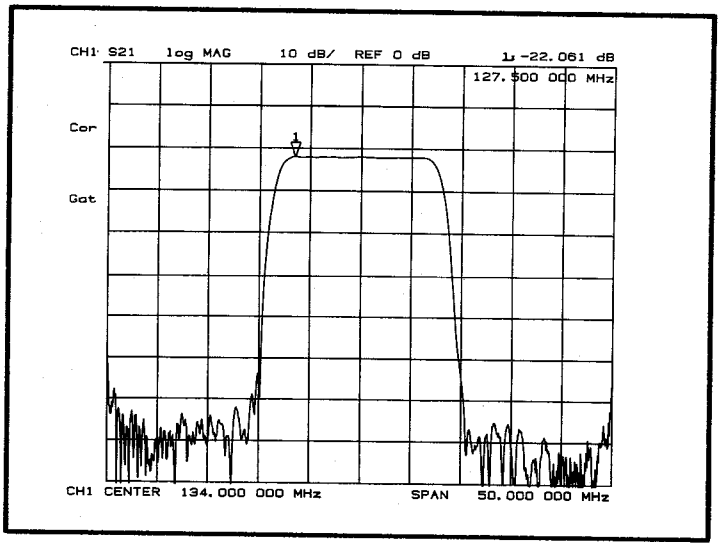

The gated frequency response shows improved stopband rejection due mostly to reduced electromagnetic feedthough as a result of the gating. Now the acoustic sidelobes are readily observed in the response.

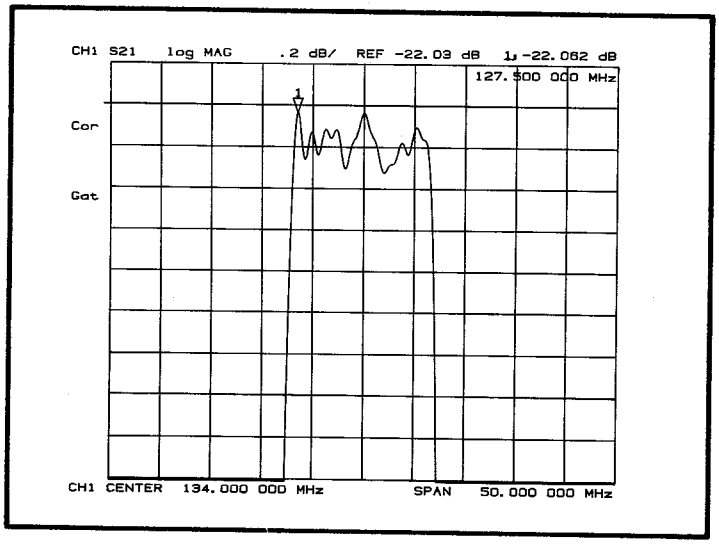

The passband of the gated response shows ripple which is due to acoustic processes within the IDT regions only. Ripples caused by electromagnetic feedthrough, triple transit, and other spurious acoustic reflections, have been suppressed by the gating. The gated response allows the user to study the acoustics in the IDT region itself without the effects of spurious time reflections. It is also useful to see what the filter response would look like if the filter was actually embedded in circuitry designed to minimize regenerative reflections and electromagnetic feedthrough. The user can, however, make these measurements in a simple 50 ohm system.

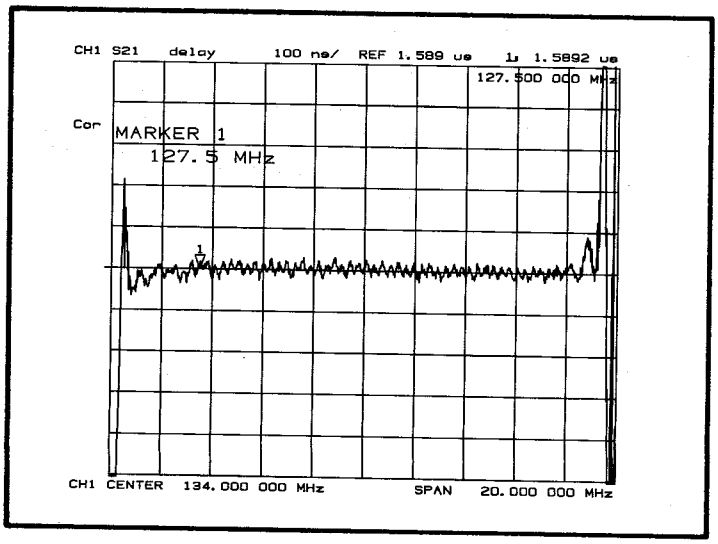

This figure shows the group delay over the passband region. The group delay is a measurement of the time delay of the filter as a function of frequency. Deviation of the group delay from a constant value over the passband region can lead to signal distortion since different frequency components are delayed by different amounts. This is especially important for broadband filters.

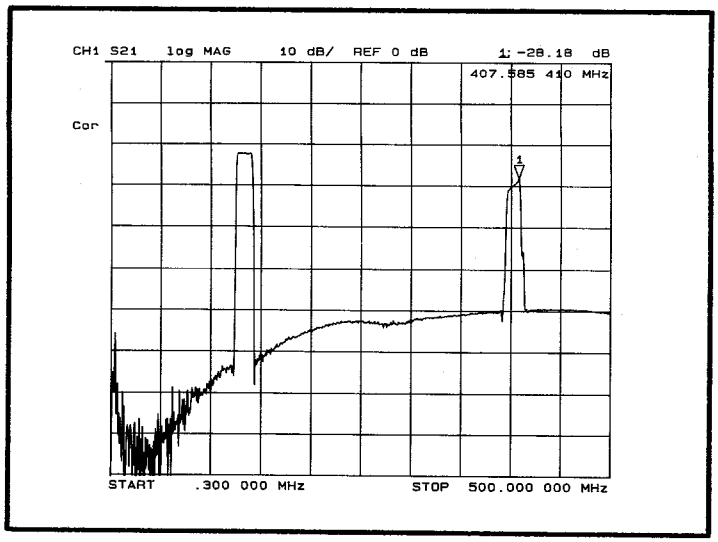

A response at three times the fundamental frequency is also observed in this particular filter. This response is produced by the inherent spatial asymmetry of the electric field produced by the split finger IDT's commonly used in brickwall filters.

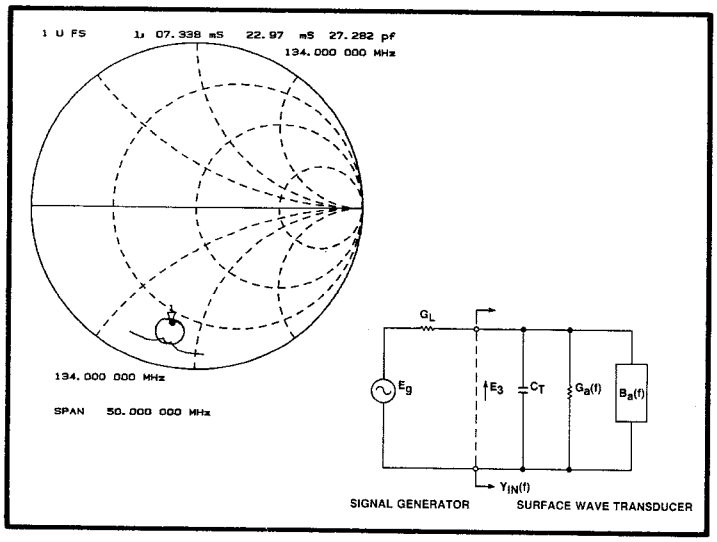

Measurement of S11 allows quick determination of the IDT radiation conductance and capacitance. The marker can be set to display impedance or admittance. In this case, admittance is dispayed. The value of capacitance or inductance is also computed and displayed. This allows equivalent circuit parameters to be measured at a glance.

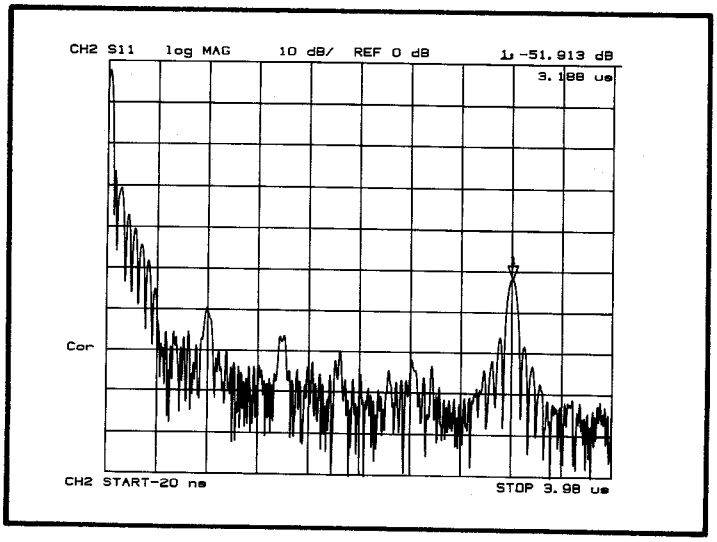

Transforming S11 frequency data to the time domain can give yet more insight into the operation of the filter. Here the main response is due to electrical reflections at the launching IDT. Marker 1 is placed on the main peak of the signal which was reflected from the receiving IDT at 3.188 uS. Again, other spurious reflections can be observed in the region between the single and double transit signals.

BULK MODE PROPAGATION PATHS

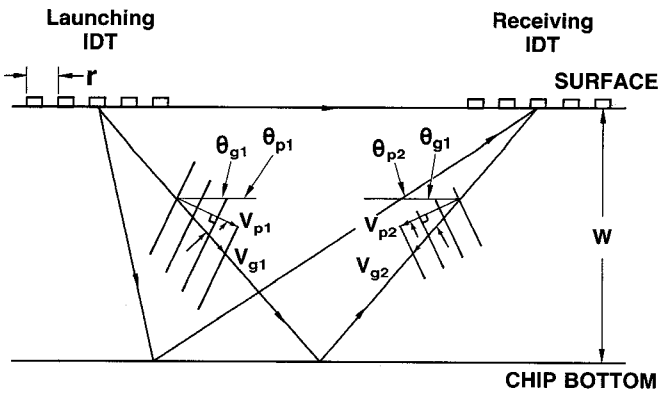

Various wave modes, other than the intended SAW, can be launched by the IDT's. Each mode propagates with a certain angle to the surface for a given crystal cut. From a knowledge of the slowness surface for a particular cut, one can compute both the group velocity and the phase velocity and their associated angles for each mode. Once these are known, the resonant frequency of the mode and the time delay can be computed. Wagers [9] has studied the various bulk modes in 128 Y LiNbO3 and has calculated the velocities and angles. Some of these modes propagate along the surface similar to the SAW. Others propagate into the bulk and reflect from the bottom of the crystal. Upon reflection, some of the energy can be coupled to a different mode. Mode conversion at the bottom of the crystal accounts for some of the more troublesome spurious signals in SAW filters built on 128 rotated Y LiNbO3.

$$fi = \frac{Vpi}{r \cos \theta pi} = \text{bulk mode resonant frequency}$$

$$T = \frac{d1}{Vg1} + \frac{d2}{Vg2} = \text{time delay of bulk mode}$$

$di = W \csc \theta gi$ = pathlength , i-1,2

$xi = W (\cot \theta_{g1} + \cot \theta_{g2})$ = horizontal distance traveled per bounce

where

Vpi = phase velocity
Vgi = group velocity
W = thickness of crystal
θpi = angle of Vpi vector
θgi = angle of Vgi vector

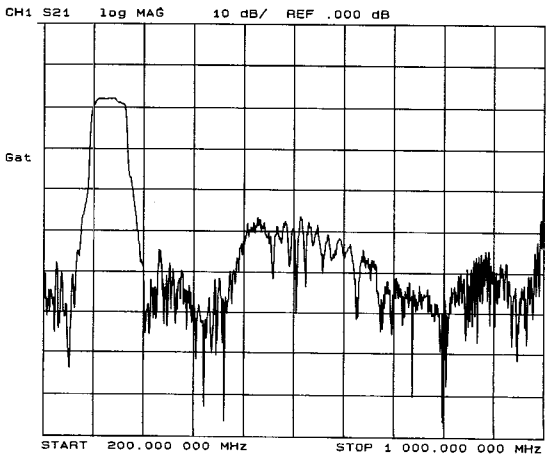

This plot shows a wide sweep of an in-line Brickwall filter. This device has a center frequency of about 300 MHz and a time delay of about 320 nS. The bulk mode spurious response can be seen in the region around 600 MHz. Most of the bulk modes are launched at frequencies higher than the SAW frequency. In fact, most of the energy is launched at about twice the frequency of the SAW.

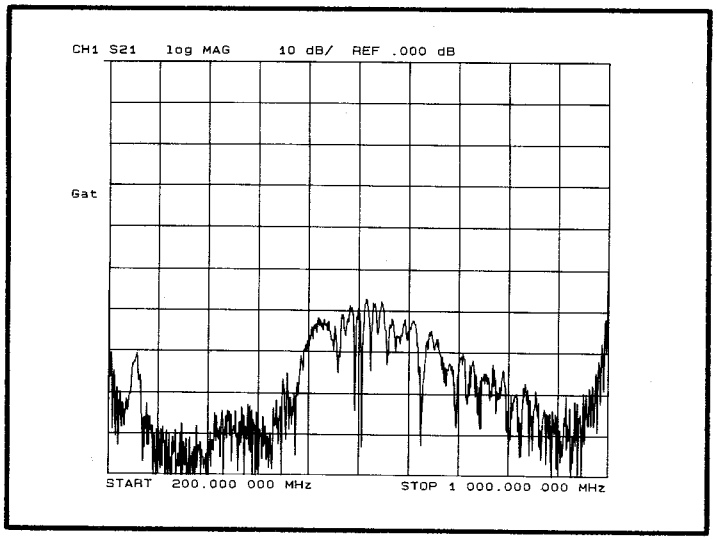

To measure these bulk modes, it is useful to coat the device surface with an acoustic absorbing material such as black wax. This suppresses the SAW but has a negligible effect on the bulk waves which propagate within the crystal. This figure shows the effect of using black wax on the surface of the device. The SAW response is completely suppressed and the bulk mode response is clearly visible. Now the user can transform to the time domain and see the time responses caused by the various bulk modes.

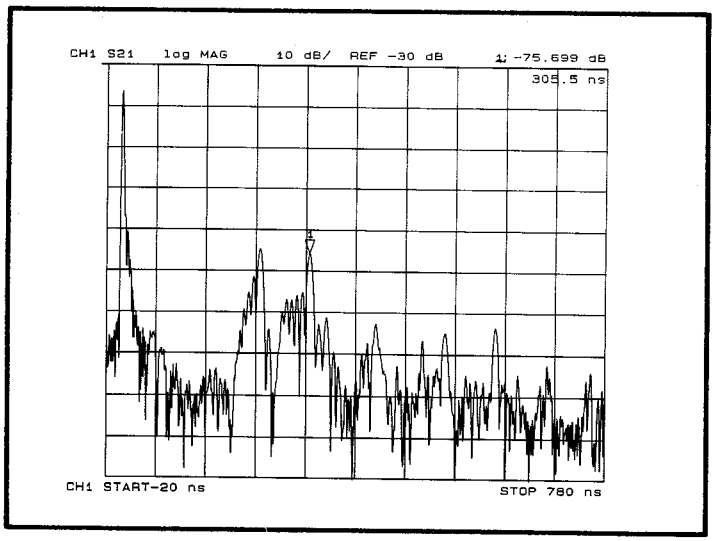

Each response corresponds to a different bulk wave or a multiple bounce of one of the waves. Note that one of the stronger responses has a time delay which is close to the SAW delay of 320 nS. This could be a potential source of frequency response degradation, especially if this energy is launched close to the SAW frequency. To see the frequency content, the user can place the gate around the time response of interest and transform back to the frequency domain.

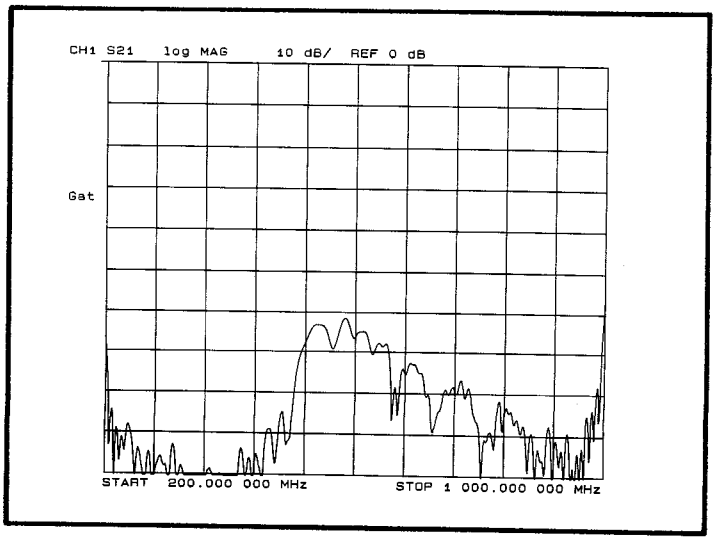

The frequency response of the two most dominant time responses is shown here. These responses account for most of the bulk mode energy that is launched in this device. Fortunately, these waves do not contain appreciable energy at the SAW frequency, but they do affect the far out stop band rejection. Without using the black wax absorber, these waves could not be observed in the presence of the stronger SAW response.

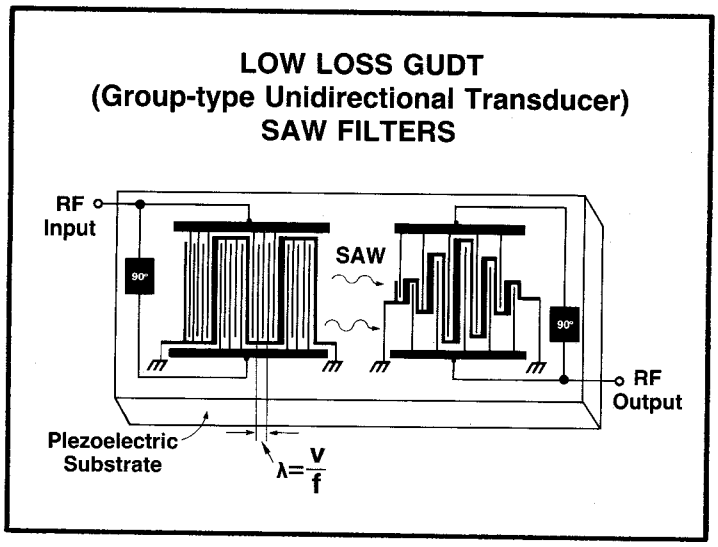

Bidirectional transducers offer precise control of filter shapes, but not without drawbacks. There is a minimum 6 dB loss due to the fact that half the energy launched is away from the output. Practical insertion losses are often 15-35 dB in order to meet demanding passband ripple specifications, since the only way to reduce triple transit ripple is to mismatch the electrical ports of the transducers. A low-loss approach to SAW filters uses unidirectional transducers. One configuration, employing group-type unidirectional transducers, is shown here. Each transducer in this case is really two phases offset on the substrate from each other by lambda/4 or 90 degrees. The two phases share the same ground electrode. This ground follows a meander pattern through the device and is alternately lambda/2 and lambda wide. This trick supplies the necessary lambda/4 offset between phases. An external electrical phase shift of 90 degrees is necessary between the two phases of each transducer, supplied by two inductors per transducer. The filter using group type transducers can be fabricated in a single, self-aligned layer with no crossovers. [8]

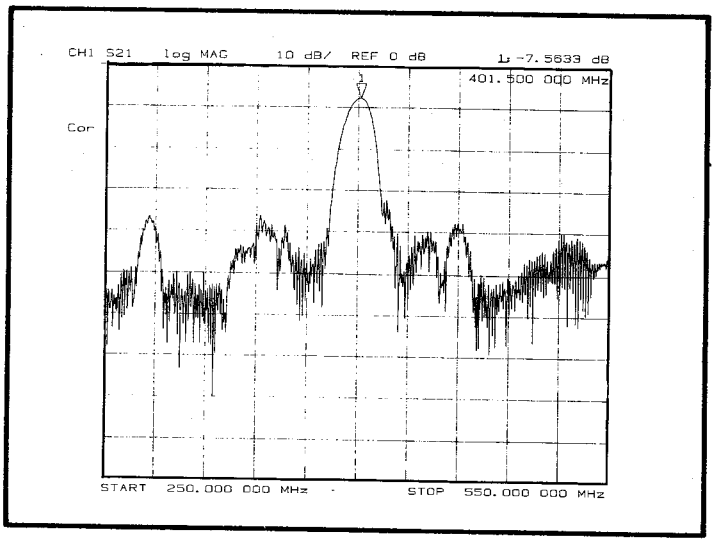

Shown here is the response of a group-type SAW filter with passband at 400 MHz. The passband minimum insertion loss is seen to be about 7.6 dB. Feedthrough is clearly visible at the 40 - 60 dB level below the input. Much of this feedthrough is test-fixture related, and will be eliminated in a properly shielded circuit board application.

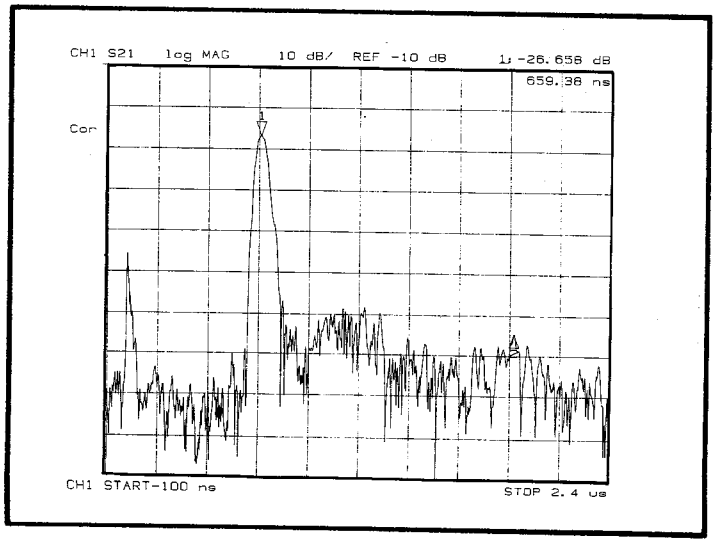

An 801-point transform to the impulse response in the time domain is shown here. The main filter response indicated by marker 1 has delay 660 nsec. The triple transit signal at marker 2 is 50 dB down, demonstrating that this type of filter design combines low loss with good triple transit suppression. At t=0 the electrical feedthrough signal is a pronounced spike. The group of features visible from ~1100-1250 nsec in the impulse response correspond to an acoustic multiple reflection within metal shield bars located between the input and output transducers, which could be eliminated at the expense of new masks. This conclusion was reached only after examination of the present time domain response.

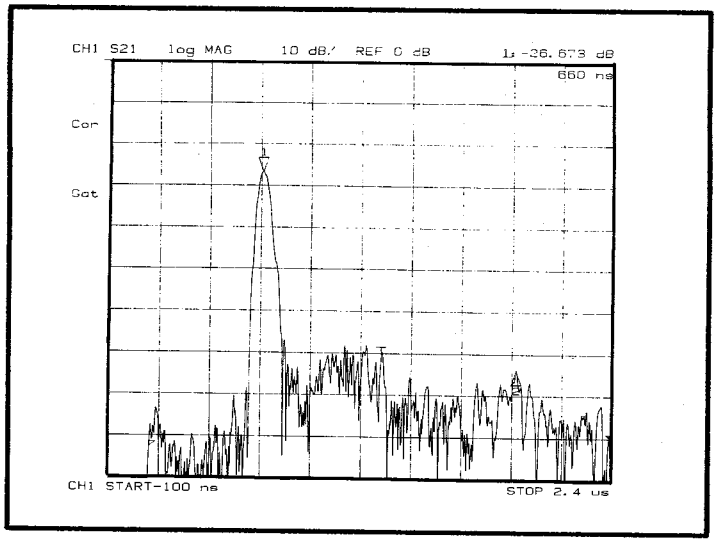

Here we use the time domain gating features of the 8753A to remove the effects of feedthrough to simulate performance in a properly shielded circuit board application.

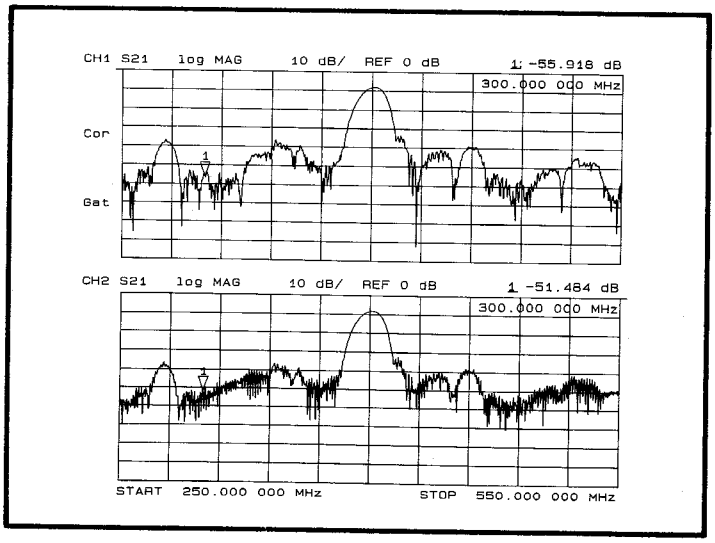

Shown here in dual channel display are the gated, retransformed frequency domain data from the previous plot in Channel 1. This simulates the circuit performance. For comparison we display in channel 2 the measured data. A critical specification for this filter is out-of-band rejection at 300 MHz. Marker 1 in both plots is set to this point. The presence of feedthrough in the response on channel 2 actually may make the SAW device's rejection at 300 MHz look better or worse. This is due to interference between the electrical and acoustic signals. The rejection due to the acoustic signal alone, which simulates circuit performance, is seen at marker 1 on Channel 1. This rejection is 55.9 dB, whereas the measured rejection is degraded to 51.5 dB by feedthrough in Channel 2.

DELAY LINES

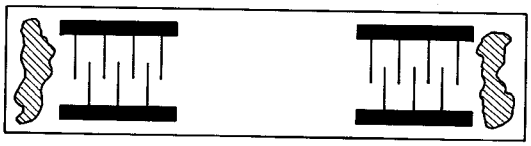

- **OSCILLATORS**
- **FM DISCRIMINATORS**
- **10 μsec DELAY IN 5 cm**

Low propagation loss for SAWs in crystals makes possible compact, convenient delay lines of 10 usec or more delay. These are highly useful in oscillator control, in FM discriminators, and other applications. The HP 8753 network analyser can be used to measure important characteristics of SAW delay lines in both the frequency domain and the time domain.

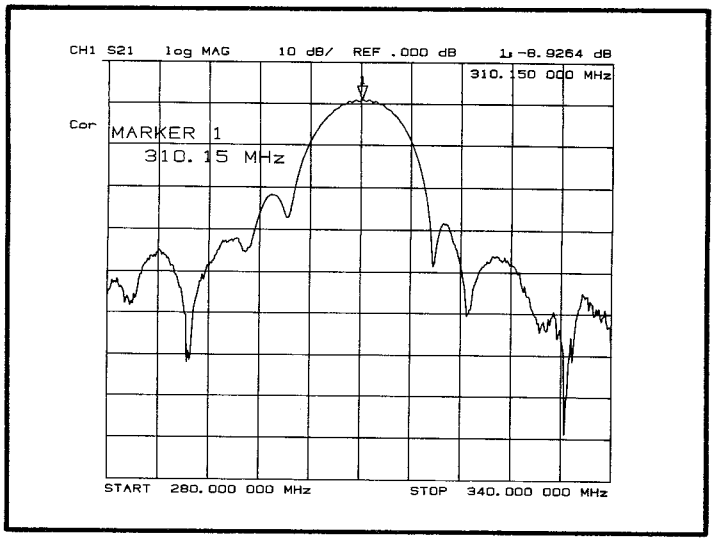

We show here the frequency response of a device with transducers similar to those employed in the low loss filter previously shown. The center frequency of this device is 310 MHz. The overall substrate length between input and output is about 10 times as great, however, giving a delay of 6.062 usec. The fixture and cable loss in the measurement are calibrated out by first doing a response calibration with a through line. Due to the long acoustic delay present in the device it is necessary to increase the resolution bandwidth and sweep time of the analyser. We have found that a bandwidth of 3 kHz and a sweep time of 2 seconds are sufficient for the 6 us device delay. Increasing the resolution bandwidth and sweep time are required to prevent anomalously high insertion loss measurements.

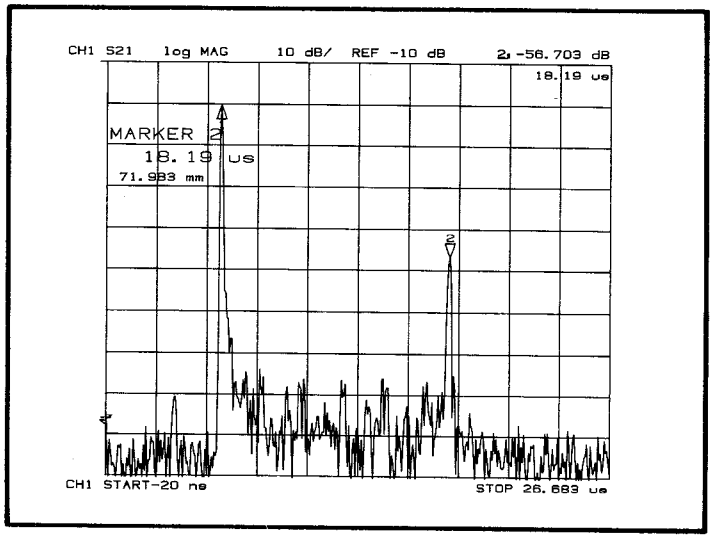

Here we use 1601 points to transform the frequency domain data into a time plot. By setting the velocity factor in the calibrate menu to .0000132 times the velocity of light (for surface waves on lithium niobate), positions of the marked time spurs are calibrated in distance on the device. The start time can be set to a small negative value to move any feedthrough signal off of the t=0 axis. If the stop time is set to some large value it is automatically set to the maximum value allowed to prevent aliasing. The figure shows no feedthrough in the long device, although both single and triple transit signals are clearly evident. The triple transit signal can be reduced by selecting optimum values for the tuning inductors of the group type unidirectional transducers. The use of 1601 points is required to prevent aliasing of the triple transit signal in the transform. The user should note that to use 1601 points, Channel 1 and Channel 2 must be decoupled and the number of points in the unused channel reduced to prevent memory overflow.

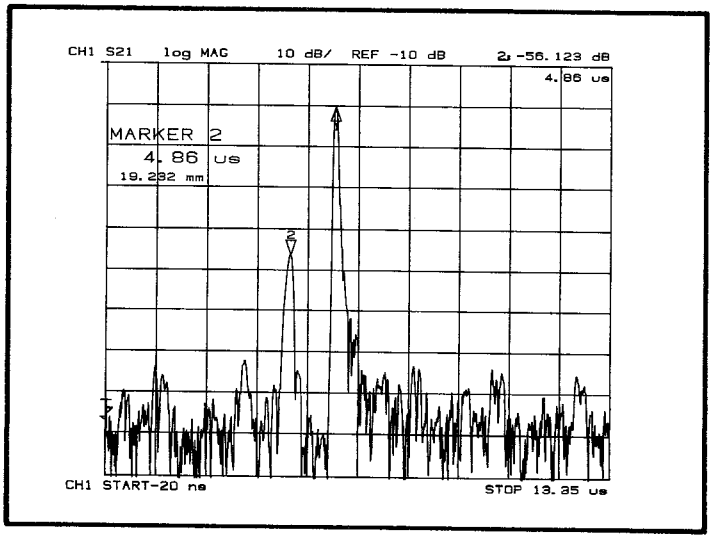

Here we show the transform using 801 points. The triple transit signal occurs, incorrectly, before the single transit signal due to aliasing. Instead of employing more points, aliasing can be eliminated by reducing the frequency span of the original measurement.

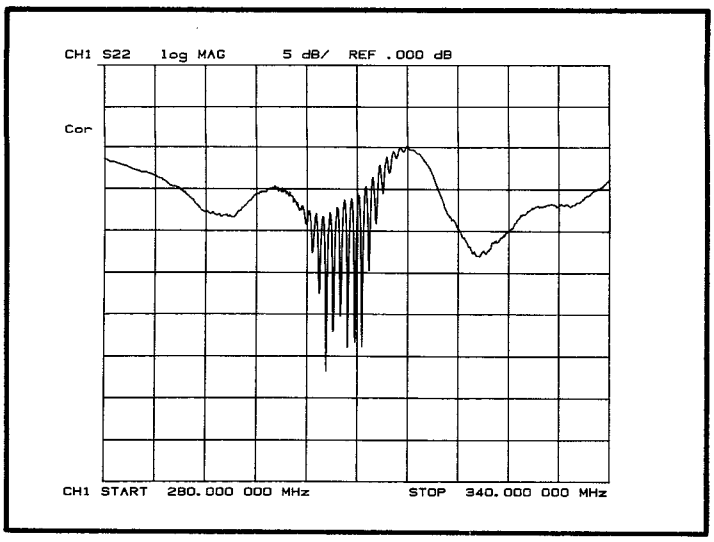

Reflected signals returning to the sending transducer are also easily measured on the HP 8753A. This figure shows S22 for a signal injected at the apodized transducer and reflecting from the unapodized transducer. The ripples indicate interference between an electrically reflected signal and an acoustically delayed signal.

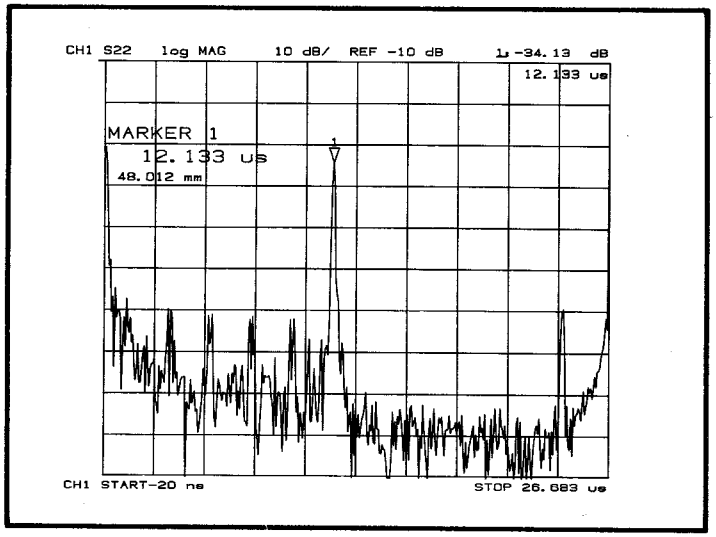

The transform of the S22 data reveals both a double and quadruple transit signal. Due to the long time span, 1601 points are required for this transform.

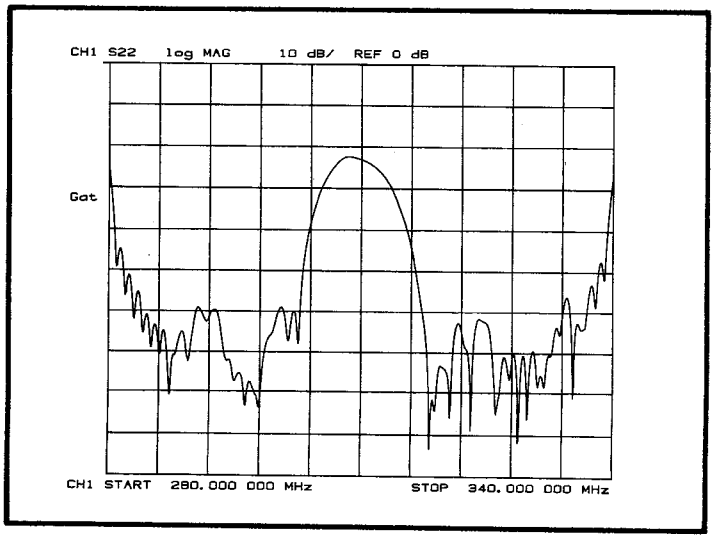

Transforming the double transit signal gives a frequency response response dominated by the filter apodization.

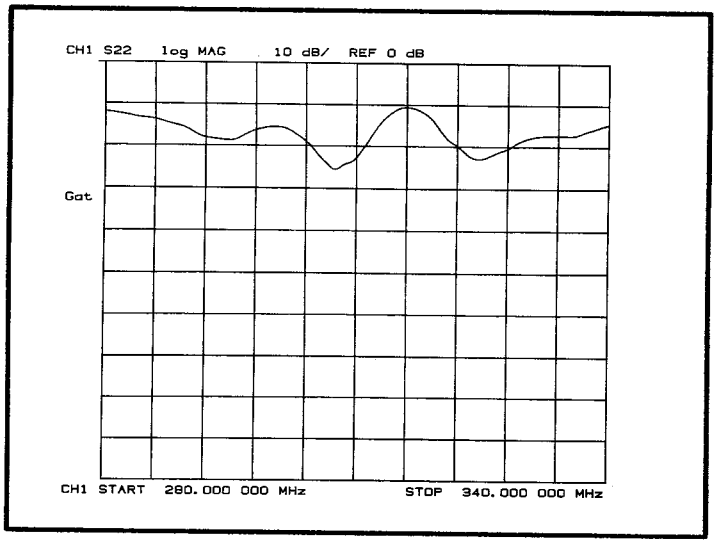

The frequency response of the signal reflected at time t=0 is more independent of frequency but shows variation due to the tuning inductors and the acoustic impedance of the transducer.

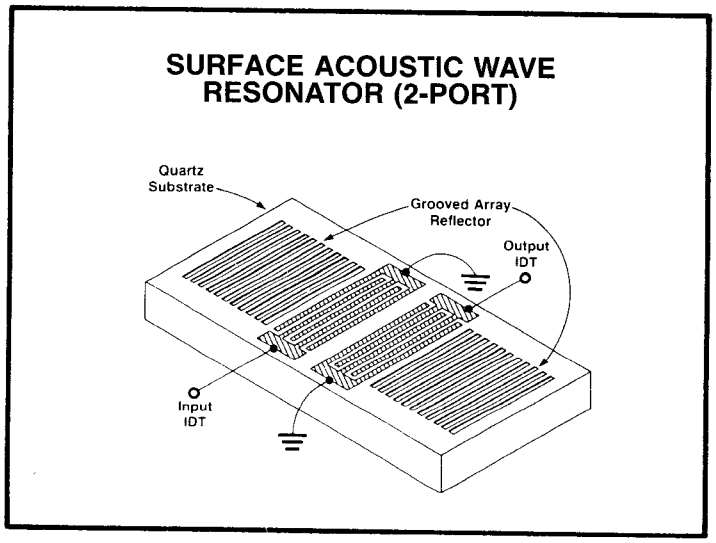

Another type of SAW device is the high-Q resonator [4,5,10]. The principal application is as the oscillator frequency control element at fundamental frequencies from ~100 MHz to ~2 GHz. Unloaded Q factors vary from 50,000 at the low end to 3,000 at the higher frequencies. These devices are usually constructed on quartz rather than on lithium niobate because of the extremely low temperature sensitivity of the former. The processing and packaging for resonators is much more difficult than for filters because of the sensitivity of the center frequency to surface contamination and process variations. The test system requirements are also different. High-Q resonator measurements demand much higher frequency accuracy, but do not need the dynamic range required in filter measurements. The HP 8753A network analyzer is again well suited for manual or automatic SAW resonator measurement.

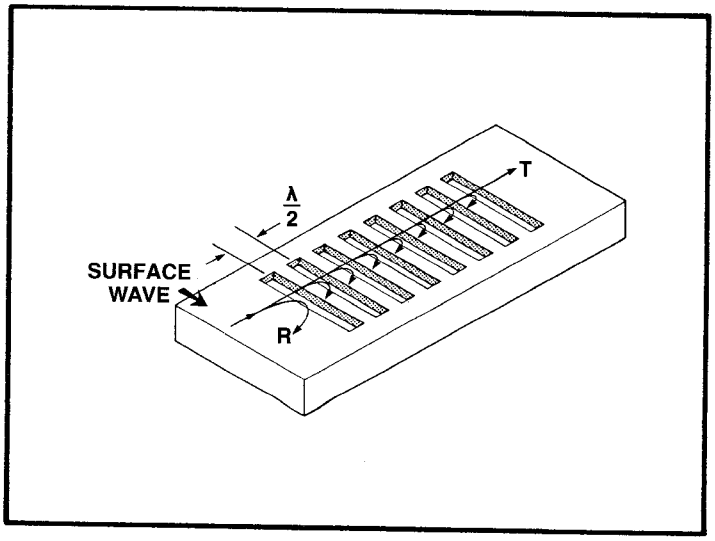

The layout of a typical SAW resonator is depicted here. The device is composed of 2 symmetric interdigital transducers (IDTs) surrounded by reflective arrays of synchronously-placed shallow grooves. The IDTs, connected to the outside world via bonding pads, serve two purposes. They act to convert electrical energy into acoustic energy and back again, and they form part of the reflective arrays. Each of the grooves (or IDT fingers) reflect a small portion of an incident acoustic wave back toward the center of the cavity. At a frequency such that the spacing between grooves (or fingers) is 1/2 wavelength, the total reflection is coherent and virtually 100% from each array. At other frequencies the combined reflection coefficient is very small.

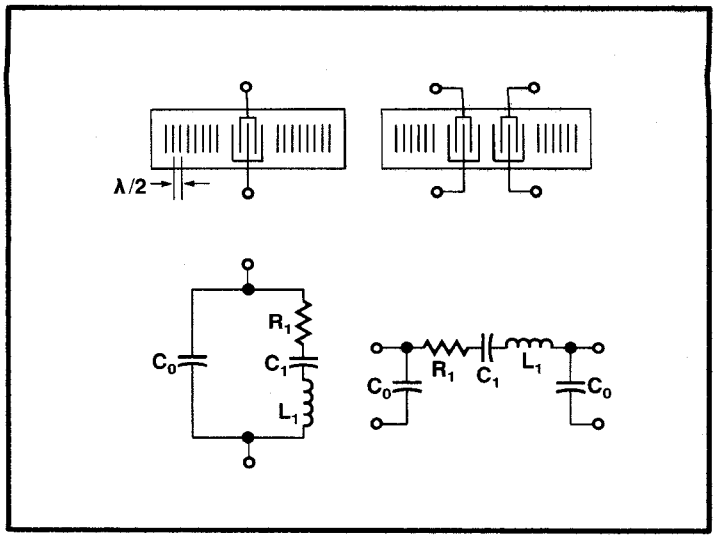

Within a few hundred kilohertz of the center frequency, this device can be modeled as a series resonant circuit. Note that both 1-port and 2-port resonator configurations are possible. The 2-port configuration is usually preferable because of the high isolation out-of-band between input and output ports. The 1-port model is the same as that for a bulk crystal resonator.

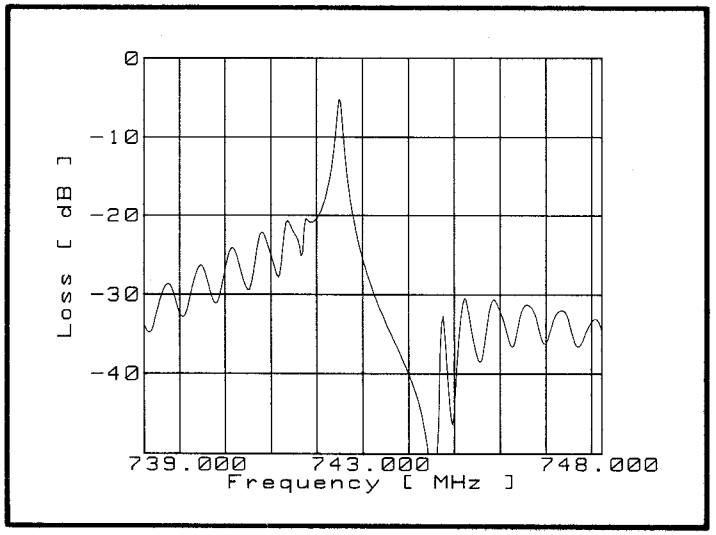

Although the resonant frequency is roughly determined by the grating and IDT periodicity, many design and processing factors can affect the exact center frequency. Optimization is required to achieve the highest Q and lowest resonant resistance at a desired frequency. Accurate mathematical models have been developed to predict the response of a SAW resonator [10]. The shoulders and ripples around this response represent the sidelobes of the reflective grating and IDT response. These ripples are important to measure and model accurately, because they give important information about the quality of the surface, the metal fingers and the grooves.

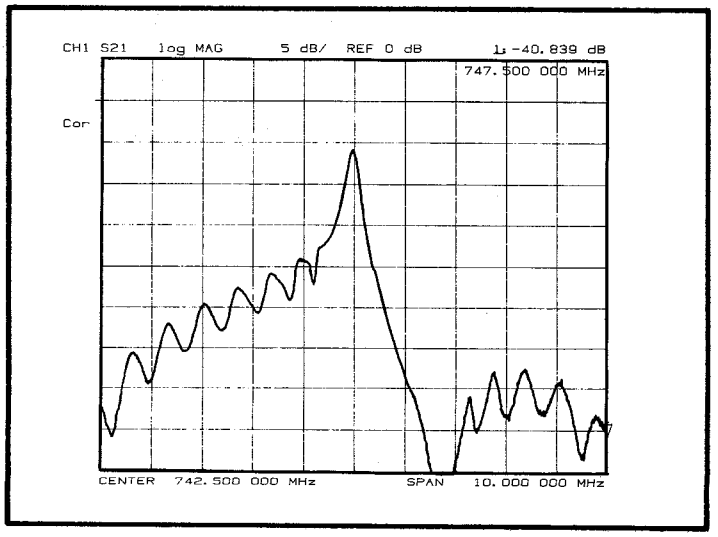

A simple, coaxial two-port fixture is used here to measure the transmission response of a SAW resonator centered at 742.5 MHz. A single thru-line calibration was done to remove the losses of the fixture and cables using the "RESPONSE" option in the calibration menu. Measuring the log of the magnitude of S21 shows good agreement with the modeled response above.

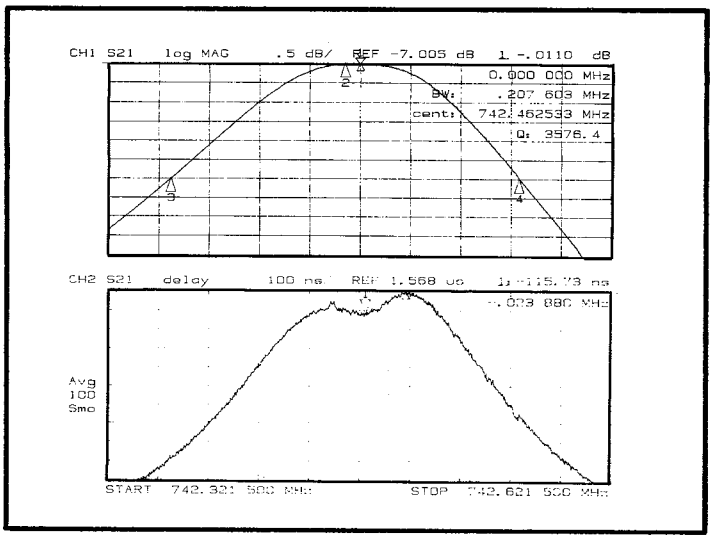

For an ideal, single-pole resonator, the loss and unloaded Q are sufficient data for an oscillator designer to predict his noise characteristics. For a real resonator, however, the resonance may be nonideal, causing unwanted noise and pulling problems. The group delay is a sensitive measure of the resonant characteristics. In this Figure, we use the GROUP DELAY display option on Channel 2 and the DUAL DISPLAY option to view the group delay response concurrently with the transmission response over a 300 KHz span. Note that the group delay response is smoothed and averaged with a factor of 100, requiring 20 seconds or so of measurement time. The response reveals a slight dip in the group delay of about 7% of the total delay, which can be read as 1.57 microseconds. The ripple in the group delay was measured by setting Marker #1 at the maximum (using the SEARCH MAX function), pressing the MARKER ZERO soft key, then moving the marker to the local minima of the dip to read the relative difference of 115.7 nSeconds. Note that the markers are independent on the two channels. This group delay dip can give rise to a lower than expected Q value on resonance, and is very difficult to detect from the amplitude data above.

LOADED Q:

$$Q_L = \frac{fo}{\Delta f}$$

UNLOADED Q:

$$\frac{1}{Q_u} = \frac{1}{Q_L} - \frac{1}{Q_{ext\ elec}} - \frac{1}{Q_{ext\ air}}$$

$$Q_{ext\ elec} = \frac{Q_L}{\tau} \qquad \tau = \text{TRANSMISSION COEFFICIENT}$$

$$Q_{ext\ air} = 66{,}700 \text{ FOR QUARTZ}$$

The loss and loaded Q allow us to derive the unloaded Q of the SAW resonator. Electrical loading is due to the 50 ohm measurement system and acoustical loading may be present if the device is operating at atmospheric pressure. The device measured above is packaged in a vacuum, and thus the unloaded Q is 7140.

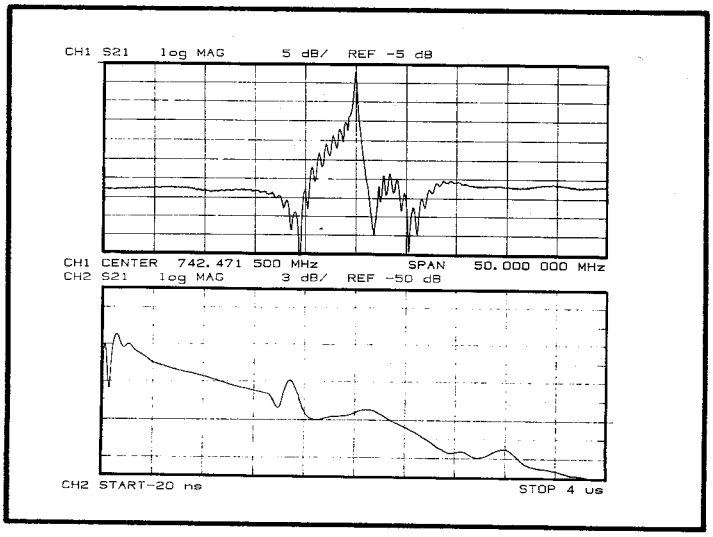

The time domain analysis capability of the HP8753A can also be very useful for analyzing SAW resonators. On the upper trace of this figure, we are viewing the amplitude response of the resonator over a 50 MHz span using 801 measurement points. On Channel 2, we have initiated the time domain capabilities in BANDPASS stimulus mode to view the Fourier transform of these data, which corresponds to the resonator impulse response. The start and stop times and scale may be set independently of the top channel. Note the sharp pulse at time zero, corresponding to direct RF feedthrough, and the basic exponential ring-down (linear on this log scale) of this impulse response. The peaks and valleys appearing in the impulse response represent acoustic reflections off of the IDTs, the reflective gratings, the ends of the quartz chip, and other physical elements of the resonator.

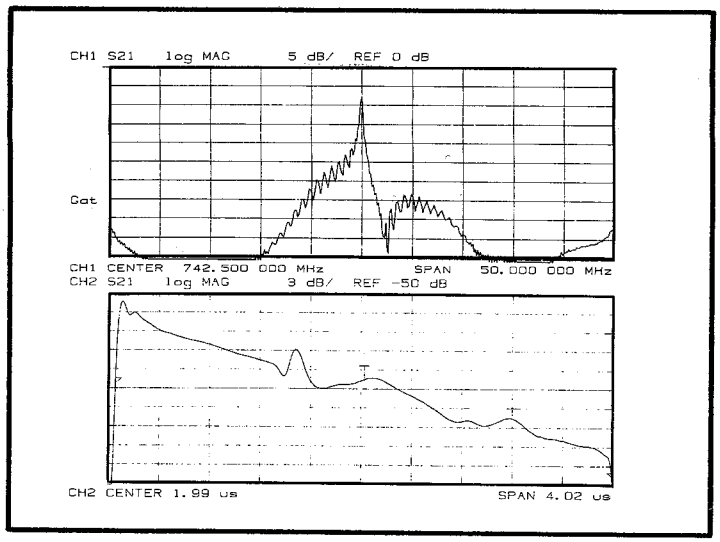

The gating feature may also be used to powerful advantage. In this figure, gates were set to remove the zero-time impulse in the time domain due to RF feedthrough. The GATE function was also turned-on in the upper, frequency domain trace to view the result. Note from comparison with the previous figure that several apparent antiresonances along the shoulders of the response were really due to destructive interference between the acoustical response and the RF feedthrough. The rises of the frequency domain response at the two ends of the span range are artifacts of the gating window and sample period.

The HP8753 is ideally suited to make the necessary measurements on SAW devices. The excellent dynamic range allows the user to measure minute detail in the response of the device. This is especially important for high insertion loss filters as is typical of brickwall filters. The internal synthesized source permits extremely accurate frequency measurements of SAW resonators. The calibration capabilities allow accurate measurement of insertion loss and impedance. The marker features allow quick access to bandwidths, frequencies, time and loss. The time domain feature is indispensable in the measurement of these devices and the 1601 point transform allows high resolution time domain information to be computed rapidly. Time domain gating and retransformation to the frequency domain enables simulation of circuit performance of devices tested in test fixtures. Automated features ease large volume testing applications.

REFERENCES

1. A. H. Cook, PHYSICS OF THE EARTH AND PLANETS. N.Y.: Wiley, 1973.

2. R.M. White and F.W. Voltmer, "Direct Piezoelectric Coupling to Surface Elastic Waves", APL 7 (Dec. 1965)

3. S. Elliott and R. Bray, "Surface Acoustic Wave Devices: Design and Measurement", Hewlett-Packard RF & Microwave Symposium, 1982-1984.

4. A.A. Oliner, ed., ACOUSTIC SURFACE WAVES. N.Y.: Springer-Verlag, 1978.

5. H. Matthews, ed., SURFACE WAVE FILTERS. N.Y.: Wiley, 1977.

6. L.F. Kinsler and A.R. Frey, FUNDAMENTALS OF ACOUSTICS, 2nd. ed. N.Y.: Wiley, 1962.

7. C.S. Hartmann, D.T. Bell, Jr., and R.C. Rosenfeld, "Impulse Model Design of Acoustic Surface Wave Filters", IEEE Trans MTT-21, 162 (1973)

8. K.Yamanouchi, F.M. Nyffeler, and K.Shibayama, "Low Insertion Loss Acoustic Surface Wave Filter Using Group-Type Unidirectional Interdigital Transducer", 1975 IEEE Ultrasonics Symposium Proceedings, IEEE Cat. #75 CHO 994-45U (1975).

9. R.S. Wagers and R.W. Cohn, "Residual Bulk Mode Levels in (YXl) 128 degree LiNbO3", IEEE Trans. on Sonics and Ultrasonics, SU-31, 168-175 (May 1984).

10. P.S. Cross, W.R. Shreve, S.S. Elliott, and R.C. Bray, "Very Low Loss SAW Resonators Using Parallel Coupled Cavities", 1982 Ultrasonics Symp. Proc., IEEE Cat #82CH1823-4, pp. 284-289.

March 1986

Printed in U.S.A.
5954-1569